

# TERRESTRIAL 3D MAPPING OF FORESTS: GEOREFERENCING CHALLENGES AND SENSORS COMPARISONS

C. R. Fol<sup>1</sup>\*, A. Murtiyoso<sup>1</sup>, D. Kükenbrink<sup>2</sup>, F. Remondino<sup>3</sup>, V. C. Griess<sup>1</sup>

<sup>1</sup> Forest Resources Management, Institute of Terrestrial Ecosystems, Department of Environmental Systems Science, ETH Zürich, Switzerland - (cyprien.fol, arnadidhestaratri.murtiyoso, verena.griess)@usys.ethz.ch

<sup>2</sup> Swiss National Forest Inventory, Swiss Federal Institute for Forest, Snow and Landscape Research WSL, Switzerland - daniel.kuekenbrink@wsl.ch

<sup>3</sup> 3D Optical Metrology (3DOM) unit, Bruno Kessler Foundation (FBK), Trento, Italy Web: <https://3dom.fbk.eu> - remondino@fbk.eu

**KEY WORDS:** Tree Georeferencing, 3D Scanning, Forest Inventory, Photogrammetry, Geometry accuracy, Point Cloud, Mixed Reality

## ABSTRACT:

Terrestrial 3D reconstruction is a research topic that has recently received significant attention in the forestry sector. This practice enables the acquisition of high-quality 3D data, which can be used not only to derive physical forest criteria such as tree positions and diameters, but also more detailed analyses related to ecological parameters such as habitat availability and biomass. However, several challenges must be addressed before fully integrating this technology into forestry practices. The primary challenge is accurately georeferencing surveyed 3D data acquired in the same location and placing them into a national projection reference system. Unfortunately, due to the forest canopy, the GNSS signal is often obstructed, and it cannot guarantee sub-metre accuracy. In this paper, we have implemented an indirect georeferencing methodology based on spheres with known coordinates placed at the forest's edge where GNSS reception was more reliable and accurate than under the canopy. We evaluated its performance through three analyses that confirmed the validity of our approach. Indeed, the accuracy of the TLS point cloud, georeferenced using our method, is within a centimetre level (4.7 cm), whereas mobile scanning methods demonstrate accuracy within the decimetre range but still less than a metre. Additionally, we have initiated the analysis of a potential future application for mixed reality headsets, which could enable real-time acquisition and visualisation of 3D data.

## 1. INTRODUCTION

The 3D mapping of forests has gained in popularity in recent decades as it enables the automation of tasks related to the derivation of forest physical parameters, which are crucial for forest inventory and ecological measurements like tree-related microhabitats (Rehush et al., 2018), and volume of standing and lying deadwood (Calders et al., 2020). Additionally, it offers the unique advantage of creating digital twins, facilitating precise parameter measurements at any time from an office, and eliminating the need for repeated visits to the forest (Murtiyoso et al., 2023). However, accurately mapping real-world forestry environments in 3D still poses challenges, both in terms of the rapid collection of reliable geometric and radiometric information (Gollob et al., 2021) and precise georeferencing of trees (Strimbu et al., 2019).

Although various 3D scanning alternatives now facilitate 3D forest reconstruction, the extreme changes in light conditions and the nearly homogeneous background texture of the forest make the data collection procedure still highly challenging with image-based methods. Therefore, range-based methods have been used more extensively, and Terrestrial Laser Scanners (TLS) have emerged as the gold standard in these 3D reconstruction technologies. Indeed, they provide accurate 3D measurements that allow for the derivation of tree physical parameters such as diameter at breast height (DBH), tree height, and tree position (Liang et al., 2016). However, TLS operates sequentially, using positioned stations to capture the environment.

Consequently, this method results in extended acquisition times for wider areas and an increased risk of data loss due to occlusions caused by the intricate elements of the forest, such as leaves, branches, and shrubs (Kükenbrink et al., 2022). As a result, alternative mobile mapping systems have gained attention due to their ability to speed up the acquisition process and reduce occlusion risks. However, it is important to acknowledge that these mobile techniques are not without their drawbacks. Mobile range-based methods often exhibit high noise levels and lower accuracy compared to TLS point clouds (Fol et al., 2023) and mobile image-based methods relying on vision-based localization techniques, such as visual odometry (VO) and Simultaneous Localization and Mapping (vSLAM), require training for data acquisition and processing tasks Di Stefano et al. (2021).

Once 3D surveyed, the representation of a forest needs to be georeferenced accurately to ensure its seamless integration into a forest inventory database or any Geographical Information System (GIS), thus enhancing collaboration efficiency among stakeholders. The georeferencing procedure has already enabled successful collaborative applications in surveying, urban planning, and the construction sectors. However, georeferencing 3D point clouds in forest environments presents a challenging task, given the poor sky visibility due to the canopy and the high probability of encountering objects that can induce multipath effects (Moore et al., 2023). Consequently, direct georeferencing within the forest is generally less accurate, especially when employing a direct georeferencing system. This involves integrating a GNSS receptor with the 3D scanner, allowing the transformation of the 3D scan coordinates from local to global

\* Corresponding author

systems. This approach contrasts with indirect georeferencing, where coordinate transformation occurs later in the office using objects with accurate and known GNSS coordinates.

The indirect georeferencing can reach higher accuracy than the direct georeferencing approach in a forest environment. Pham et al. (2023) compared the direct and indirect georeferencing approaches and determined that while the indirect approach demands more time due to setting up additional GNSS fixed points (at least 3), it can achieve higher accuracy down to the centimetre level if the fixed points' positioning geometry is optimal. In fact, Pham et al. (2023) proved that better results are achieved with targets positioned at varying heights and evenly distributed across the entire area of interest. Nevertheless, in forests it is hard to place objects with such optimal geometry, hence Verma and Yadav (2023) developed a method where checkerboard targets were placed inside of the forest and measured by a Total Station (TS) placed at the entrance of the forest. Similarly, Oveland et al. (2018) developed a method based on 3 spheres measured with a TS at the centre of the forest plot. An alternative method for precise georeferencing of terrestrial 3D data involves its use in conjunction with aerial imagery (Strimbu et al., 2019). However, this approach can be excessive as it necessitates processing data from drones and aligning it with terrestrial data. Furthermore, to the best of our knowledge, no method has been developed using only GNSS receivers to georeference the ground control points. This could greatly facilitate the task since operating a GNSS antenna is much easier compared to a TS or other surveying instrument.

To sum up, accurately mapping real-world forestry environments in 3D still poses challenges, both in terms of 3D data collection and precise georeferencing. Responding to these challenges is crucial for the accurate mapping of forests (e.g., for forest inventory and biodiversity monitoring purposes), as well as supporting new technologies such as Mixed Reality (MR) which can enable remote collaboration between professionals in the field and in the office.

Driven by these needs, this research work has three main objectives:

1. Develop an indirect georeferencing method designed explicitly for forestry point clouds acquired under the canopy using static TLS. This method will address the challenges posed by obstructed GNSS signals, allowing for precise spatial referencing of the acquired data.
2. Evaluate and compare several mobile terrestrial 3D sensors in a forest environment with state-of-the-art static TLS techniques. The goal is to determine whether portable image- and range-based solutions can achieve comparable geometric accuracy for accurately geolocating trees in almost GNSS-denied areas while offering faster data acquisition.
3. Assess the feasibility of using indirect georeferencing with a MRH (Mixed Reality Headset) to display and collect 3D content in the forest. This study will tackle the issue of precise alignment between the physical environment and virtual content in areas with obstructed GNSS signals.

To answer these three objectives, the paper is organised as follows. In Section 2, a detailed presentation is provided regarding the materials and the forest plot chosen for the measurement

campaign. Additionally, the methods employed for data collection and processing are described. In Section 3, firstly, a comparison is conducted to evaluate the accuracy of georeferencing TLS with the proposed indirect method and the direct georeferencing approach. A comparison involving the indirect georeferencing of mobile 3D scanners is detailed. Last but not least, the limitations and potential of MRH systems for the future are discussed. In Section 4, the paper is concluded.

## 2. METHODS

### 2.1 Material and Study Area

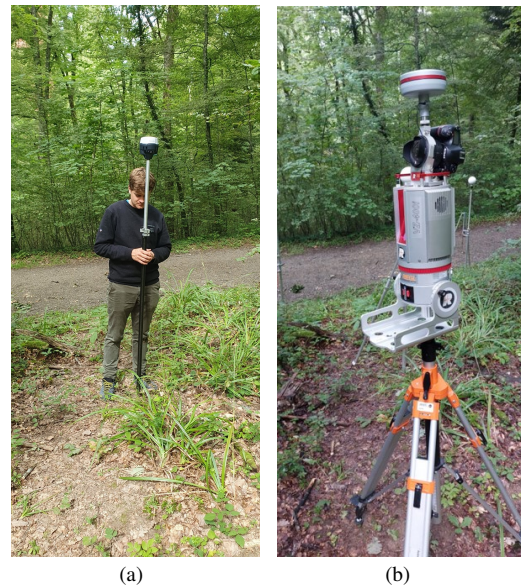


Figure 1. GNSS surveying equipment: a multi-band RTK GNSS receiver Reach RS2+ by EMLID (a) and a RIEGEL VZ-i GNSS RTK Receiver mounted on top of the TLS.

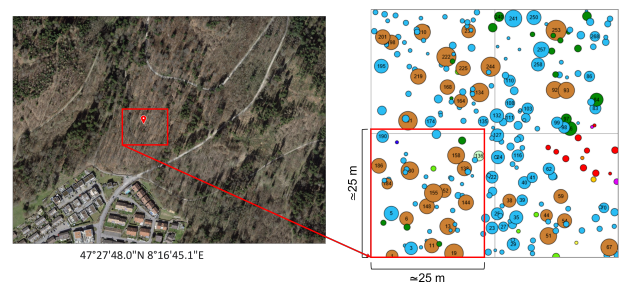


Figure 2. Top view of the measured area: orthophoto image (on the left) and tree distribution Map within the Baden marteloscope (on the right)

The employed GNSS equipment is shown in Figure 1, and the 3D mapping systems are detailed in Table 1. These survey equipments were operated over a 2 days measurement campaign in the summer months in the region of Baden, Switzerland and cover a 25x25 [m] forest area. The selected forest area is part of an existing marteloscope, as shown in Figure 2. A marteloscope is a designated forest plot spanning 1 ha, specifically designed for educating foresters and other interested stakeholders regarding silvicultural practices. They provide a framework for in-forest training in the selection and marking

	TLS	LSHH	SVHH	MRH
Manufacturer	Riegl	Leica Geosystems / GeoSLAM	FBK	Microsoft
Name	VZ400i	BLK2GO / ZEB Horizon	GuPho	Hololens 2
Measurement	Range-based	Range-based	Image-based	Range-based
Acquisition	Stationary	Mobile	Mobile	Mobile
Range (m)	800	25 / 100	*	3.5
Positioning	RTK GNSS	SLAM	vSLAM	SLAM

Table 1. Comparative table of data acquisition material: Terrestrial Laser Scanner (TLS), Laser Scanner Hand-Held (LSHH), Stereo-vision Hand-Held (SVHH), Mixed Reality Headset (MRH). \*It is a triangulation-based system with a baseline of 20 cm, and the range depends on the accuracy threshold you set.

of trees for management purposes. In Figure 2, the distribution of tree species within the Marteloscope is depicted. It is noticeable that the Marteloscope is a mixed forest, dominated by beech (*Fagus Sylvatica*) and oak (*Quercus*) trees, indicated by light blue and brown dots, respectively.

## 2.2 Data Collection

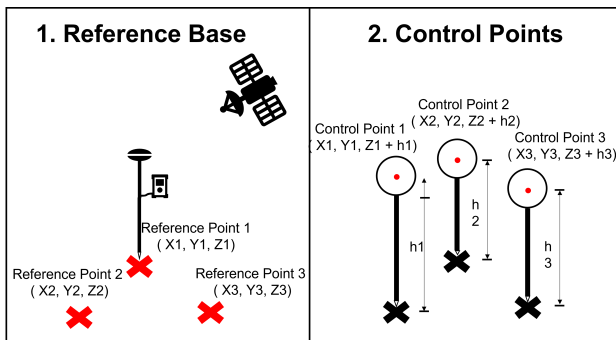


Figure 3. Visual representation of the preparation phase

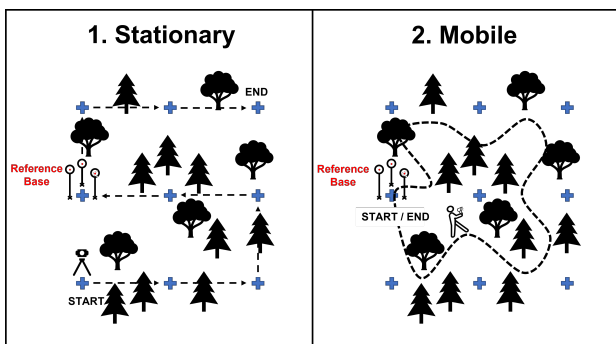


Figure 4. Visual representation of the acquisition phase

The data collection process consisted of several phases, starting with the preparation phase, as illustrated in Figure 3, which included the following steps:

1. Establishing a reference base in an area with stable GNSS signal reception. This involved measuring at least 3 fixed points using a GNSS antenna capable of RTK processing. In our case, the multi-band RTK GNSS receiver Reach RS2+ by EMLID (Emlid Tech Kft., Budapest, Hungary), with centimetre precision, was employed (see Figure 1(a)). These points were physically marked on the ground using nails.

2. Set up of control points for the point cloud georeferencing, each with a sphere mounted at a known height with the help of surveying poles. These spheres were positioned above the previously measured nails, thus achieving the georeferencing accuracy of the GNSS-measured points of approximately a few centimetres. Three ground control points were located outside the forest and two other spheres were used as check points inside the forest.

Once the preparation phase was completed, the acquisition phase could begin. The illustration of this phase is shown in Figure 4, and the following are the steps involved:

1. Perform a scan of the entire forest area using the static TLS. The acquisition process involves moving the TLS device along a predefined grid, which includes the reference base as one of the grid nodes.
2. Utilise mobile 3D solutions, both image- (Torresani et al., 2021; Menna et al., 2022) and range-based, to survey the forest area, starting and ending the acquisition at the reference base established during the preparation phase. This is illustrated in Figure 5.



Figure 5. Picture of the reference base and the mobile mapping system (GuPho) ready to begin the surveying.

## 2.3 Indirect Georeferencing Approach

The method used in this paper to georeference the datasets acquired in the field was a two-step indirect georeferencing (Pham et al., 2023). Using CloudCompare version 2.13 alpha) (Lague et al., 2013) software, the corresponding world coordinates of the centres of the three reference spheres (left spheres from Figure 6) were matched. This procedure relied on the CloudCompare tool called 'align,' which allowed for the automatic identification of sphere centres and matching them to 3D points. In

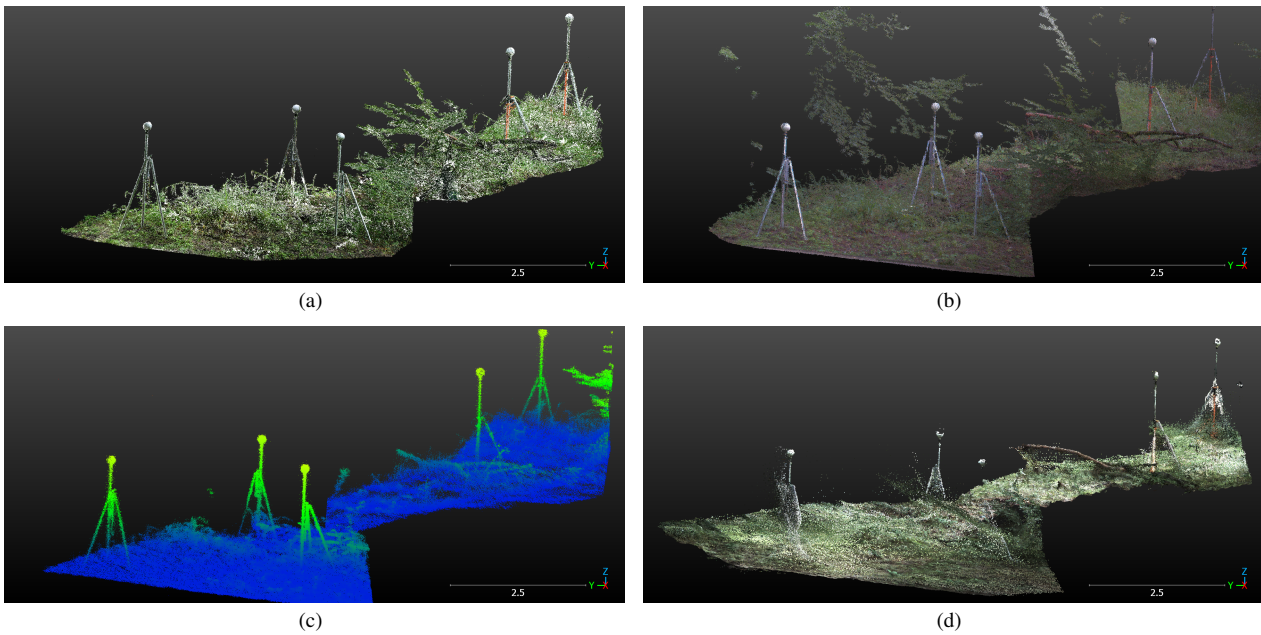


Figure 6. Dataset illustration of the extracted spheres used for the indirect georeferencing approach from the TLS point cloud (a), BLK2GO point cloud (b), Zeb Horizon point cloud (c), and GuPho point cloud (d).

our case, the known radius of the sphere was 7 cm. The 'auto-adjust scale' option was unchecked since each of the respective methods already generated scaled results, and the rest was kept as default.

## 2.4 Data Analysis

First, all the acquired point clouds were georeferenced using the aforementioned procedure.

For the comparative analyses of the geometric accuracy between the indirect and direct approaches 3.1 and among the mobile mapping applications 3.2, the five spheres placed in the scene were manually extracted from each point cloud. The coordinates of the sphere centres were retrieved using the Automatic Sphere Detection tool, and residuals' mean and sigma were computed using the formula below:

$$\mu_{res.} = \frac{1}{N} \sum_{i=1}^N |y_{GNSS_i} - y_{scan_i}| \quad (1)$$

$$\sigma_{res.} = \sqrt{\frac{\sum_{i=1}^N (y_{GNSS_i} - y_{scan_i})^2}{N}} \quad (2)$$

where  $y_{GNSS_i}$  represents the coordinates of the checkpoint measured by the GNSS receiver, and  $y_{scan_i}$  represents the coordinates of the checkpoint measured in the 3D point clouds.

Regarding the third analysis, the CloudCompare plugin, 3DFIN (3D Forest INventory) (Cabo et al., 2018), was used with the following basic parameters: stripe limit within 0.7-10 m and a pruning intensity of 5. Then, a MATLAB script was employed to match each tree's position to the most likely position in the other dataset using a nearest neighbour distance search. The results were then plotted and verified visually. After verification, the root mean square error (RMSE) for each position was calculated.

## 3. RESULTS AND DISCUSSION

### 3.1 Indirect Georeferencing Evaluation

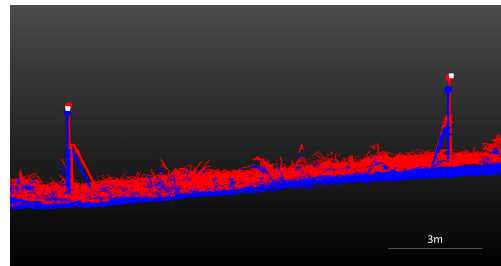


Figure 7. Visual comparison of the accuracy of the indirect georeferencing (red) and direct georeferencing (blue) of the TLS point clouds. White square are the true position of the sphere centre measured with a GNSS receivers

	Residuals Mean			Residuals Sigma
(cm)	X	Y	Z	3D
<b>Indirect</b>	2.6	6.3	4.4	4.7
<b>Direct</b>	3.4	10.2	17.5	12.0

Table 2. Comparative table of bias and accuracy for the indirect and direct georeferencing of a TLS point cloud.

In Figure 7 a noticeable difference was already apparent with the two spheres serving as checkpoints located on the right in the point cloud. The centre positions of these spheres should align with the white points in Figure 6 (GNSS reference values) and the TLS point cloud georeferenced using the indirect approach appeared closer to the reference values of the GNSS receiver. This is quantified in Table 2, which illustrates that the residual sigma of the indirect georeferencing method is lower than half of a decimetre (4.7 cm). In contrast, the direct georeferencing, showed deviations exceeding a decimetre (12.0 cm).

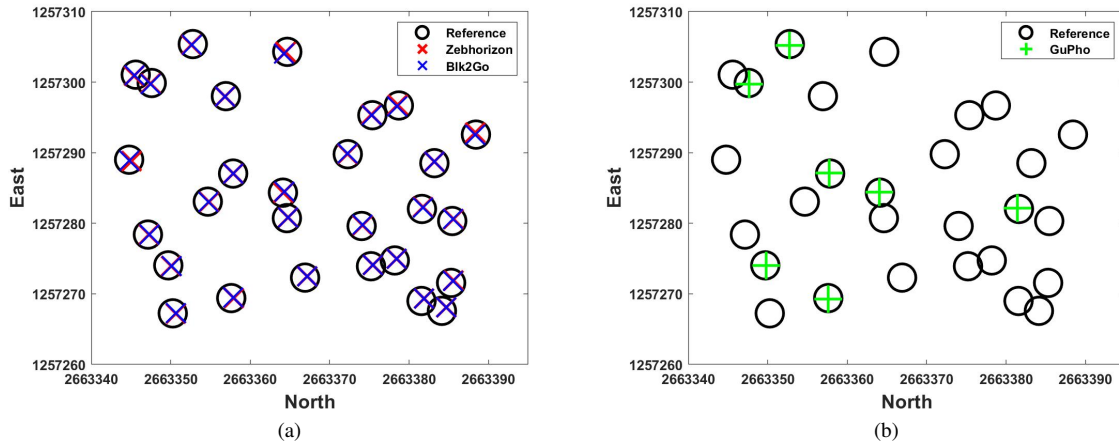


Figure 8. Plot of the position of trees detected in range-based surveying (29 trees) (a) and in image-based surveying (7 trees) (b). Axes scales are in meters.

Upon closer examination of the residuals mean for each coordinate, it becomes evident that, in terms of planar coordinates, the georeferencing methods fall within a similar order of magnitude. However, when considering the altimetric dimension (Z), it is noted that direct georeferencing exceeds a decimetre in magnitude (17.5 cm), while indirect georeferencing remains below one decimetre (4.7 cm).

A discrepancy at the decimetre level is significant; however, it is important to acknowledge that only two spheres served as checkpoints, making it challenging to generalise these results in a statistical context. This discrepancy can be attributed to the accumulation and propagation of errors while transporting the TLS from one station to another, potentially leading to a drift effect. Nevertheless, the RIEGL TLS RTK module measured the position for each scan and filtered out only those with good positioning quality. So, explaining a decimetre-level discrepancy solely by this is not realistic. An additional potential source of error could be linked to the one-week time lag between the TLS acquisition and the GNSS position measurements. Besides changes in satellite geometry, when driving nails into the forest ground, there are external disturbances that could occur due to the evolution of plant and animal activity or meteorological events.

In summary, our indirect georeferencing method can be regarded as satisfactory with regard to the direct georeferencing method. This responds to objective 1 of this work. Our indirect georeferencing method can be now applied to the mobile mapping point clouds. This aspect is the focus of the subsequent section.

### 3.2 Mobile 3D Mapping Application

(cm)	Residuals Mean			Residuals Sigma
	X	Y	Z	3D
<b>TLS</b>	2.6	6.3	4.4	4.7
<b>BLK2GO</b>	6.2	8.6	22.6	14.9
<b>Zeb Horizon</b>	6.8	10.8	28.6	18.7
<b>GuPho</b>	12.8	10.4	5.1	10.4

Table 3. Comparative table of the bias and accuracy of mobile mapping point clouds and the TLS one.

(cm)	Residuals RMS		
	X	Y	Planar
<b>BLK2GO</b>	22.6	18.9	20.8
<b>Zeb Horizon</b>	23.1	19.6	21.4
<b>GuPho</b>	8.6*	11.9*	10.4*

Table 4. Comparative table of indirect georeferencing accuracy for the mobile mapping point cloud and the reference static mapping TLS. \*only 7 trees were detected in the GuPho Point Cloud whereas 29 in the others

In Table 3, when considering the mobile mapping devices, the mean residuals in the y-coordinates appear to be of the same order of magnitude. However, the two other coordinates show large differences between the image-based 3D surveying (GuPho) and the range-based 3D surveying (BLK2GO and Zeb Horizon). The difference in the x-coordinate falls below a decimetre in magnitude and can be considered not significant for forest inventory tasks, while for the Z-coordinate, the difference exceeds a decimetre in magnitude. Nevertheless, this discrepancy was expected, given that visual positioning systems inherently offer greater resistance to error propagation thanks to the loop closure, particularly in the Z-coordinate. This is further reflected in the residuals, where GuPho has the smallest value (10.4 cm), closest to TLS (4.7 cm).

The final ranking of mobile mapping devices is as follows: GuPho was ranked first, followed by BLK, and Zebhorizon was last. This ranking validated the initial expectations that both range-based surveys would demonstrate similar levels of accuracy based on the technical specifications. Interestingly, the image-based system outperformed the accuracy of the range-based system. This can be explained by the high level of noise inherent in the range-based method. GuPho, on the other hand, is capable of maintaining a low level of noise in the 3D reconstruction process, thanks to a visual interface that provides live feedback on the Ground Sampling Distance (GSD) and motion blur during the acquisition and thresholds on triangulated points (Menna et al., 2022).

However, a similar limitation concerning the statistical significance of the results was encountered, as in the previous section. This limitation stemmed from the challenge of establishing a fixed GNSS positioning antenna solution under the forest canopy, allowing for the setup of only two checkpoints. To address



Figure 9. 3D mesh of HoloLens spatial mapping for the forest plot (grey) with tree detected in colour and their associated DBH

this limitation, the positions of other natural elements present in the TLS scan can be utilised. In particular, in the next section the positions of trees served as a means for a secondary verification of this ranking.

In Table 4, the image-based point cloud (GuPho) achieved an accuracy for each column that was at least 2 times smaller than that of the range-based ones (BLK2GO and ZebHorizon). Furthermore, it is interesting to note that there were no significant differences between the X and Y coordinates. This means that there is little to no systematic error on the planimetric axes.

However, this result needs to be nuanced because, as depicted in Figure 5, it was only possible to acquire data for 7 trees in the point cloud (Figure 8(b)). Overall, it confirms the preliminary ranking obtained with the checkpoints. However, it also highlighted the difficulty of the image-based method in navigating areas with dense vegetation, due to the different GuPho trajectory, whereas the mobile laser scanners were able to explore these areas and scanned 29 trees without problems (Figure 8(a)). This aligns with the earlier findings of Di Stefano et al. (2021), indicating that the image-based system provides very detailed 3D point clouds at the expense of a slower and more complex acquisition procedure.

This conclusion potentially opens the door to additional mobile mapping systems. Moreover, during the data acquisition, a Mixed Reality Headset was used, and its spatial mapping capabilities are described in the following section.

### 3.3 Mixed Reality Application

Regarding the MRH used for data acquisition, as depicted in Figure 9, the georeferenced spheres were absent from the reconstructed 3D model, rendering it impossible to apply our indirect georeferencing method. This outcome can be attributed to the small diameter of the pole on which the spheres were positioned. Additionally, the monochromatic white colour of the spheres presented challenges in their detection when using the HoloLens spatial mapping system.

Nevertheless, the forest mesh acquired contained valuable information. As demonstrated in Figure 9, the position and diameter of 12 trees were successfully acquired using the same procedure as in the previous analysis. Tree detection proved

to be more efficient than with the image-based point cloud, primarily due to the design of the helmet, which leaves the user's hands-free to manipulate branches and shrubs obstructing the view. These results are highly promising, and our next challenge is to find an alternative method for georeferencing the point cloud. For example, we could explore the possibility of merging the depth sensor with the two colour cameras. This integration would enhance the recognition of spheres and potentially reduce Z-drift, as observed in the case of image-based sensors. Additionally, rather than relying on spheres, we could consider utilising georeferenced automatic coded targets attached to trees. This has already been investigated by Mokroš et al. (2021).

## 4. CONCLUSION

In this study, we addressed the critical challenge of georeferencing in 3D forest scans, a pivotal step in forest inventories and biodiversity conservation. The research centred on evaluating the performance of indirect georeferencing of forest 3D point cloud, utilising only three ground control points, with direct georeferencing methods.

The findings, as presented in Tables 2, 3, and 4, shed light on the effectiveness of these approaches. Favourable results were achieved in georeferencing TLS 3D point clouds, with deviations well below a decimetre (4.7 cm). Further evaluations were conducted by applying the indirect approach to mobile mapping devices, including one image-based (GuPho) and two range-based (BLK and ZebHorizon) 3D surveyings. It was observed that the image-based surveying consistently outperformed the range-based surveyings in terms of residuals, with the smallest deviations noted in the residual sigma. This reaffirmed the expectation that visual positioning systems demonstrate resistance to drift, especially in the z-coordinate. Subsequently, the investigation extended to tree positioning within the point clouds, and the results were consistent with the rankings obtained with checkpoints. However, the image-based method exhibited limitations in dense vegetation areas and could only capture seven trees in the point cloud. In contrast, range-based methods managed to acquire more than 29 trees, making them more suitable for forestry applications. Nevertheless, hybrid technologies like MRH, which combine range-based and image-based sensors, hold promise for the future.

The study explored the use of MRH for data acquisition, revealing promising opportunities. Although challenges with georeferencing arose due to the absence of georeferenced spheres in the captured point cloud, tree positions remained accessible using the MRH. This innovative approach, offering users hands-free capabilities, enabled efficient navigation through obstructed forest environments, surpassing the capabilities of handheld devices.

In summary, this research demonstrates that indirect georeferencing is a reliable and precise alternative to direct methods. Furthermore, the findings encourage the application of the georeferencing method to explore various mobile mapping systems. These insights underscore the importance of considering the specific requirements of forest mapping when selecting mapping devices. Finally, the development of a robust georeferencing methodology, combined with the integration of advanced 3D scanning techniques and visualisation technologies, holds the potential to transform forest inventory practices. By harnessing the capabilities of 3D sensor technology and overcoming georeferencing challenges, this research paves the way for new and improved approaches to accurate forest assessment and monitoring.

## 5. ACKNOWLEDGEMENTS

The authors are grateful to Prof. Dr. Benedikt Soja for providing us with the GNSS equipment and to Prof. Dr. Marc Pollefeys for lending us the Microsoft HoloLens 2 during the data acquisition.

## References

- Cabo, C., Ordóñez, C., López-Sánchez, C. A., Armesto, J., 2018. Automatic dendrometry: Tree detection, tree height and diameter estimation using terrestrial laser scanning. *International Journal of Applied Earth Observation and Geoinformation*, 69, 164-174.
- Calders, K., Adams, J., Armston, J., Bartholomeus, H., Bauwens, S., Bentley, L. P., Chave, J., Danson, F. M., Demol, M., Disney, M., Gaulton, R., Krishna Moorthy, S. M., Levick, S. R., Saarinen, N., Schaaf, C., Stovall, A., Terry, L., Wilkes, P., Verbeeck, H., 2020. Terrestrial laser scanning in forest ecology: Expanding the horizon. *Remote Sensing of Environment*, 251, 112102.
- Di Stefano, F., Torresani, A., Farella, E. M., Pierdicca, R., Menna, F., Remondino, F., 2021. 3D Surveying of Underground Built Heritage: Opportunities and Challenges of Mobile Technologies. *Sustainability*, 13(23).
- Fol, C. R., Kükenbrink, D., Rehus, N., Murtiyoso, A., Griess, V. C., 2023. Evaluating state-of-the-art 3D scanning methods for stem-level biodiversity inventories in forests. *International Journal of Applied Earth Observation and Geoinformation*, 122, 103396.
- Gollob, C., Ritter, T., Kraßnitzer, R., Tockner, A., Nothdurft, A., 2021. Measurement of Forest Inventory Parameters with Apple iPad Pro and Integrated LiDAR Technology. *Remote Sensing*, 13(16).
- Kükenbrink, D., Marty, M., Bösch, R., Ginzler, C., 2022. Benchmarking laser scanning and terrestrial photogrammetry to extract forest inventory parameters in a complex temperate forest. *International Journal of Applied Earth Observation and Geoinformation*, 113, 102999.
- Lague, D., Brodu, N., Leroux, J., 2013. Accurate 3D comparison of complex topography with terrestrial laser scanner: Application to the Rangitikei canyon (N-Z). *ISPRS Journal of Photogrammetry and Remote Sensing*, 82, 10-26.
- Liang, X., Kankare, V., Hyyppä, J., Wang, Y., Kukko, A., Haggrén, H., Yu, X., Kaartinen, H., Jaakkola, A., Guan, F., Holopainen, M., Vastaranta, M., 2016. Terrestrial laser scanning in forest inventories. *ISPRS Journal of Photogrammetry and Remote Sensing*, 115, 63-77.
- Menna, F., Torresani, A., Battisti, R., Nocerino, E., Remondino, F., 2022. A Modular and Low-Cost Portable Vslam System for Real-Time 3d Mapping: from Indoor and Outdoor Spaces to Underwater Environments. *The International Archives of the Photogrammetry, Remote Sensing and Spatial Information Sciences*, XLVIII-2/W1-2022, 153–162.
- Mokroš, M., Mikita, T., Singh, A., Tomaščík, J., Chudá, J., Wezyk, P., Kuželka, K., Surový, P., Klimánek, M., Zieba-Kulawik, K., Bobrowski, R., Liang, X., 2021. Novel low-cost mobile mapping systems for forest inventories as terrestrial laser scanning alternatives. *International Journal of Applied Earth Observation and Geoinformation*, 104, 102512.
- Moore, A., Rymer, N., Glover, J. S., Ozturk, D., 2023. Predicting gps fidelity in heavily forested areas. *2023 IEEE/ION Position, Location and Navigation Symposium (PLANS)*, 772–780.
- Murtiyoso, A., Holm, S., Riihimäki, H., Krucher, A., Griess, H., Griess, V. C., Schweier, J., 2023. Virtual forests: a review on emerging questions in the use and application of 3D data in forestry. *International Journal of Forest Engineering*, 0(0), 1-14.
- Oveland, I., Hauglin, M., Giannetti, F., Schipper Kjörsvik, N., Gobakken, T., 2018. Comparing Three Different Ground Based Laser Scanning Methods for Tree Stem Detection. *Remote Sensing*, 10(4).
- Pham, D., Long, N., Tinh, L., Tran, H., 2023. Indirect georeferencing in terrestrial laser scanning: One-step and two-step approaches. *Advances in Geospatial Technology in Mining and Earth Sciences*, Springer International Publishing, 171–186.
- Rehus, N., Abegg, M., Waser, L. T., Brändli, U.-B., 2018. Identifying Tree-Related Microhabitats in TLS Point Clouds Using Machine Learning. *Remote Sensing*, 10(11).
- Strimbu, B. M., Qi, C., Sessions, J., 2019. Accurate Georeferencing of Trees with No or Inaccurate Terrestrial Location Devices. *Remote Sensing*, 11(16).
- Torresani, A., Menna, F., Battisti, R., Remondino, F., 2021. A V-SLAM Guided and Portable System for Photogrammetric Applications. *Remote Sensing*, 13(12).
- Verma, M. K., Yadav, M., 2023. Registration, Georeferencing and Processing of Multiple Laser Scans Acquired by Terrestrial Laser Scanner for Estimating Tree Morphological Parameters. *ISPRS Annals of the Photogrammetry, Remote Sensing and Spatial Information Sciences*, X-4/W1-2022, 737–742.